(9) Cabane, B.; Duplessix, R. *J. Phys. (Les Ulis, Fr.)* **1987**, *48*, 651.
(10) Hayakawa, K.; Ohyama, T.; Maeda, T.; Satake, I.; Kwak, J. C. T. *Langmuir* **1988**, *4*, 481.
(11) Dubin, P. L.; Oteri, R. *J. Colloid Interface Sci.* **1983**, *95*, 453.
(12) Dubin, P. L.; Davis, D. D. *Macromolecules* **1984**, *17*, 1294.
(13) Dubin, P. L.; Davis, D. D. *Colloids Surfaces* **1985**, *13*, 113.
(14) Dubin, P. L.; Rigsbee, D. R.; McQuigg, D. W. *J. Colloid. Interface Sci.* **1985**, *105*, 509.
(15) Dubin, P. L.; McQuigg, D. W.; Rigsbee, D. R. *Polym. Prep. (Am. Chem. Soc. Div. Polym. Chem.)* **1986**, *27* (1), 420.
(16) Dubin, P. L.; Rigsbee, D. R.; Fallon, M. A.; Gan, L. M. *Macromolecules* **1988**, *21*, 2555.
(17) Dubin, P. L.; Thé, S. S.; McQuigg, D. W.; Gan, L. M.; Chew, C. H. *Langmuir* **1989**, *5*, 89.
(18) Dubin, P. L.; Gan, L. M.; Chew, C. H. *J. Colloid Interface Sci.* **1989**, *128*, 566.
(19) Dubin, P. L.; Skelton, J.; Curran, M., Sudbeck, E., in preparation.
(20) Koppel, D. E. *J. Chem. Phys.* **1972**, *57*, 4814.
(21) Strege, M. A.; Dubin, P. L. *J. Chromatogr.* **1989**, *463*, 165.
(22) Lin, F. M. Calgon Corp., private communication.
(23) (a) Provencher, S.; Hendrix, J.; de Maeyer, L. *J. Phys. Chem.* **1978**, *69*, 4273. (b) Provencher, S. *Makromol. Chem.* **1979**, *180*, 20. (c) Nicoli, D. F. Private communication.
(24) Morrison, I. D.; Grabowski, E. F.; Herb, C. A. *Langmuir* **1985**, *1*, 496.
(25) In the Nicomp software, "fit error" is obtained from the sum of the squares of the errors between the fitted autocorrelation curve and the measured one, normalized with respect to particle size, while the "residual" is the coefficient obtained for the decay constant corresponding to an infinitely large particle, and is frequently attributed to dust "events".
(26) Huglin, M. B. In *Light Scattering from Polymer Solutions*; Huglin, M. B., Ed.; Academic Press: New York, 1972; p 165.
(27) Burkhardt, C. W.; McCarthy, K. J.; Parazak, D. P. *J. Polym. Sci., Polym. Lett. Ed.* **1987**, 25, 209.
(28) Imae, T.; Ikeda, S. *Colloid Polym. Sci.* **1984**, *262*, 497.
(29) Mankowich, A. M. *J. Phys. Chem.* **1954**, *58*, 1027.
(30) Kushner, L. M.; Hubbard, W. D. *J. Phys. Chem.* **1954**, *58*, 1163.
(31) Dubin, P. L.; Principi, J. M.; Smith, B. A.; Fallon, M. A. *J. Colloid Interface Sci.* **1989**, *127*, 558.
(32) See, for example: Elias, H.-G. in ref 26, Chapter 9.
(33) For reviews, see: (a) Tsuchida, E.; Abe, K. In *Interactions between Macromolecules in Solution and Intermacromolecular Complexes*; Advances in Polymer Science 45; Springer-Verlag: Berlin, 1982. (b) Smid, J.; Fish, D. In *"Encyclopedia of Polymer Science and Technology*; Wiley-Interscience: New York, 1988, Vol. 11, p 720.
(34) (a) Kharenko, O. A.; Kharenko, A. V.; Kasaikin, V. A.; Zezin, A. B.; Kabanov, V. A. *Polym. Sci. USSR (Engl. Transl.)* **1980**, *21*, 3009 (translation of *Vysokomol. Soyed.* **1979**, *A21*, 2726). (b) Kabanov, V. A.; Zezin, A. B. *Makromol. Suppl.* **1984**, *6*, 259.
(35) Dubin, P. L.; Vea, E. M. Y.; Thé, S. S. *Abstracts*, Colloid and Surface Science Division; National Meeting of the American Chemical Society, Miami Beach, FL, Sept 1989; *Langmuir*, in press.
(36) Fallon, M. A. Thesis, Purdue University, 1986.
(37) (a) Dubin, P. L.; Murrell, J. M. *Macromolecules* **1988**, *21*, 2291. (b) Strege, M. A.; Dubin, P. L.; Flinta, C. D.; West, J. S. In *Downstream Processing and Bioseparation*; Hamel, J.-F. P., Hunter, J. B., Sikdar, S. K., Eds.; ACS Symposium Series 419; American Chemical Society: Washington, DC, 1990; p 158.

Flow and Viscoelastic Properties of Xanthan Gum Solutions

Michel Milas and Marguerite Rinaudo*

Centre de Recherches sur les Macromolécules Végétales, CNRS, BP 53 X, 38041 Grenoble Cedex, France

Magali Knipper and Jean Luc Schuppiser

Rhône Poulenc, Centre de Recherches d'Aubervilliers, 52, Rue de la Haie Coq, 93308 Aubervilliers Cedex, France. *Received May 16, 1989; Revised Manuscript Received October 31, 1989*

ABSTRACT: This paper concerns the rheological behavior of an unpasteurized sample of xanthan as a function of the polymer concentration and of the conformation of the polysaccharide. The evidence of critical concentrations (C^* and C^{**}) is discussed from steady shear and dynamic experiments. The behavior of the xanthan solutions is characteristic of polymeric solutions without any evidence of gellike character in contrast with the results obtained previously on commercial samples.

Introduction

Xanthan is a bacterial polysaccharide which has been widely studied in recent years. However, the results diverge on many aspects such as the nature of the ordered structures[1] or the influence of the substituents on its properties in solution.[2] In contrast, an apparent agreement exists about the conformational transition in solution and its dependence with temperature, ionic strength, and substituent contents. In fact, only a few studies take into account the existence of two different ordered conformations in solution (native and renatured) which modify the hydrodynamic and rheological properties but not the position of the conformational transition;[3] aggregates which are generally present in commercial xanthan samples lead to the same behavior.

Concerning the conformation of xanthan in solution, the chain model usually adopted now is that of a wormlike chain characterized by an intrinsic persistence length either around 500 Å if we adopt the single helix as ordered conformation[4] or around 1200 Å in the case of a double helix.[5]

A first approach of the viscoelastic properties of xanthan gum was made by Thurston et al. in 1981.[6] These authors showed that the same relaxation processes are responsible for both the steady and the oscillatory flow behavior and were sufficient to describe how the viscoelasticity changes with both shear rate and frequency and how the steady flow viscosity changes with shear rate.

0024-9297/90/2223-2506$02.50/0

Later, from a wide range of rheological experiments, Ross-Murphy et al.[7,8] found that solution viscoelasticity was drastically modified by changing the counterion of the polyelectrolyte and by treatment with urea, although in all cases, the local ordered structure was unaffected. They conclude that, in aqueous solution, xanthan may be regarded as a highly extended wormlike chain interacting by noncovalent association to develop a weak-gel network, which is readily reversible under shear. For example, the so-called Cox–Merz rule is no more obeyed even in semidilute solutions and at lower frequencies and shear rates. A similar behavior was found by Cuvelier and Launay.[9] These authors deduced from flow and viscoelastic properties different concentration regimes in xanthan gum solution in which different master curves are obtained due to a change in the density of junction zones of the elastic network formed by side by side associations. The influence of salt, temperature, and strain effects on the structure of xanthan solution from xanthan dried powder and a pasteurized fermentation broth has been studied by Rochefort and Middleman[10] using oscillatory and steady shear experiments. Their conclusions are very similar to the previous ones. Nevertheless, a master curve of dynamic properties covering 6 decades of frequency has been obtained in highly saline solution and the frequency/temperature superposition allows characterization of the conformational transition induced by temperature change. More recently, steady and dynamic shear properties of aqueous polymer solutions, including xanthan, have been published.[11] These studies have been carried out for xanthan concentration lower than 1 g/L and for frequencies lower than 1 rad/s. In these conditions, in absence of salt, they found that measurements follow the Cox–Merz rule in low shear rate and frequency regions and that the dynamic results agree qualitatively with the trend predicted by the Zimm molecular model. A master curve is obtained by means of the shift factor M/CRT as suggested by Ferry.[12] Nevertheless, the rheological properties of xanthan depend not only on the nature of the counterion and salt contents but also on postfermentation treatments like pasteurization and drying which form in xanthan commercial samples large and irreversible aggregates.[13] From these samples, gellike behavior is well demonstrated from the previous studies,[6-10] and it is clear that the structure of these solutions cannot be described by a classical polymer entanglement concept.

In this paper, a xanthan from an unpasteurized broth was used, taking care to avoid aggregation and to preserve the native conformation during purification.[3] Using this well-characterized xanthan, steady shear and dynamic experiments were performed in the native and renatured conformations in dilute and semidilute regimes in the range of polymer concentration up to 5 g/L (i.e, $C[\eta] < 65$).

Experimental

Material. An unpasteurized broth from Rhône Poulenc (Aubervilliers, France) was diluted in 0.01 M NaCl solution to an estimated concentration of about 1 g/L. It was filtered through 8-, 3-, 1.2-, and 0.8-μm Millipore filters successively and centrifugated for 2 h at 20000g. Afterward, NaCl (60 g/L) was added. The xanthan was precipitated by addition of ethanol to a concentration of 50% (v/v). The precipitate was then washed successively with ethanol/water mixtures from 70% (v/v) to 100%. The xanthan powder was dried at 25 °C under vacuum for 2 days. Afterward it was stored in ambient conditions until it reached equilibrium; its degree of hydration measured by thermogravimetry with a Setaram balance (Model G70) was then 12%. This method for the recovery of xanthan from the broth preserves the native ordered structure (N) and gives the sodium salt with the minimum of aggregation. The solutions were prepared by dissolving the required amount of purified xanthan in 0.01 M NaCl solution. Half of the volume of these solutions was heated at 80 °C (1 min) and cooled to 20 °C. After this cycle, the xanthan is in its renatured conformation (R).[3] Then, 9% (v/v) of 1 M NaCl solution was added into the heated and nonheated solutions in order to reach a final NaCl concentration equal to 0.1 M. The lowest xanthan concentrations were obtained by dilution of a more concentrated polymeric solution with 0.1 M NaCl. Nevertheless, it was checked that the results were independent of the solution preparation technique (direct dissolution or dilution of a more concentrated solution).

Table I
Characteristics of Xanthan in Dilute Solutions[a]

conformation	$\bar{M}_w$	A_2, mL g^{-2} mol	$[\eta]_{\dot\gamma\to 0}$, mL/g	k'	C^*, g/L	C^{**}, g/L
native	5.25×10^6	0.6×10^{-3}	10 300	0.45	0.126	0.78
renatured	5.25×10^6	0.7×10^{-3}	13 200	0.46	0.100	0.60

[a] Note: C^* and C^{**} are obtained from Figure 2.

Techniques. The degrees of pyruvate substitution and acetylation were measured by ^{1}H NMR. Dried xanthan was dissolved in 5×10^{-3} M sodium acetate solution (in D_2O) at a polymer concentration of about 5 g/L. Sodium acetate (5×10^{-3} M) was used as an internal standard. The spectra were obtained with a Bruker WP 100 spectrometer at 85 °C. The OH signals were suppressed by irradiation. A total of 200 scans were accumulated with a repetition time of 7 s and a sweep width of 1125 Hz. The acetate and pyruvate yields were expressed as an average number per side chain.

Intensities of light scattered from the xanthan solutions (polymer concentrations usually lower than C^* varied from 0.02 to 0.15 g/L in 0.1 M NaCl) were measured at an angle of 6° with a low-angle laser light scattering apparatus (Chromatix KMX 6) at 25 °C; clarification of xanthan solutions was achieved by filtration throguh 0.22-μm Millipore filters. The value of dn/dc was taken to be 0.155 mL/g.[3] The main characteristics of the polymer used are the following: $\bar{M}_w = 5.25 \times 10^6$; pyruvate and acetate contents equal 0.25 and 0.50, respectively. Flow curves were obtained with two viscometers: the Contraves low-shear LS30 ($\dot\gamma$ from 0.017 to 128 s^{-1}) and the Carrimed CS 50 ($\dot\gamma$ from 0.02 to 2500 s^{-1}) using different coaxial cylinder and cone-plate systems.

Dynamic measurements were performed with the Rheometrics fluid spectrometer (RFS) (rate from 10^{-2} to 10^2 rad/s and strain from 1 to 50%) using a coaxial cylinder ($R_1 = 16$ mm, $R_2 = 17$ mm, and $h = 32$ mm). The torque has to be greater than 5×10^{-3} N·m.

All the rheological experiments were performed in 0.1 M NaCl and at constant temperature (25 °C).

Results and Discussion

1. Characterization of Xanthan Solutions in the Newtonian Regime. The weight-average molecular weight, $\bar{M}_w$, the intrinsic viscosities, $[\eta]$, determined in the Newtonian regime, the second virial coefficients, A_2, and the Huggins constant, k', are given in Table I for xanthan in the native and renatured conformations. The polydispersity was determined by steric exclusion chromatography and found to be 1.5.[14]

Viscosities in the Newtonian plateau and their dependence on shear rate were determined on the two conformations in the range of polymer concentration from 0.0125 to 5 g/L; a few experimental results obtained for the relative viscosity are given in Figure 1.

The values of the specific viscosities in the Newtonian regime (reached only for xanthan concentration lower than 2.5 g/L) as a function of the overlap parameter $C[\eta]$ in a logarithmic plot are given in Figure 2. A unique curve

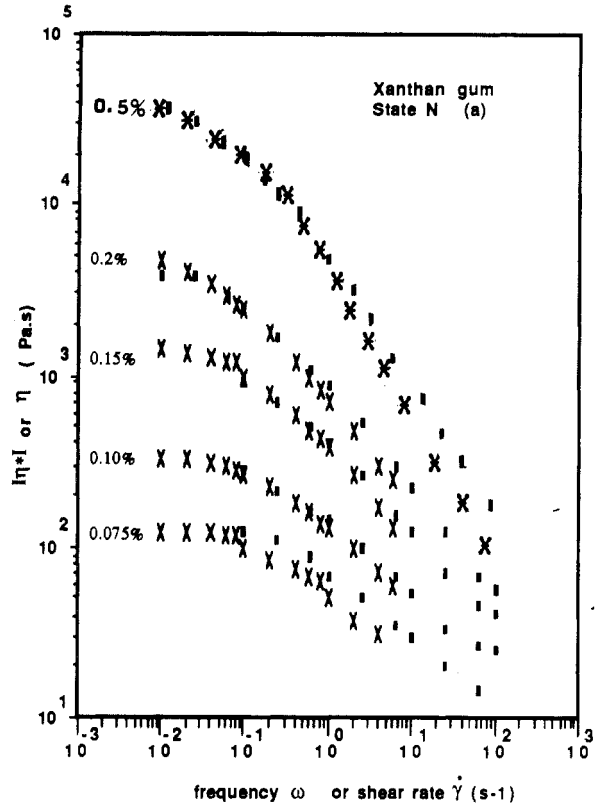

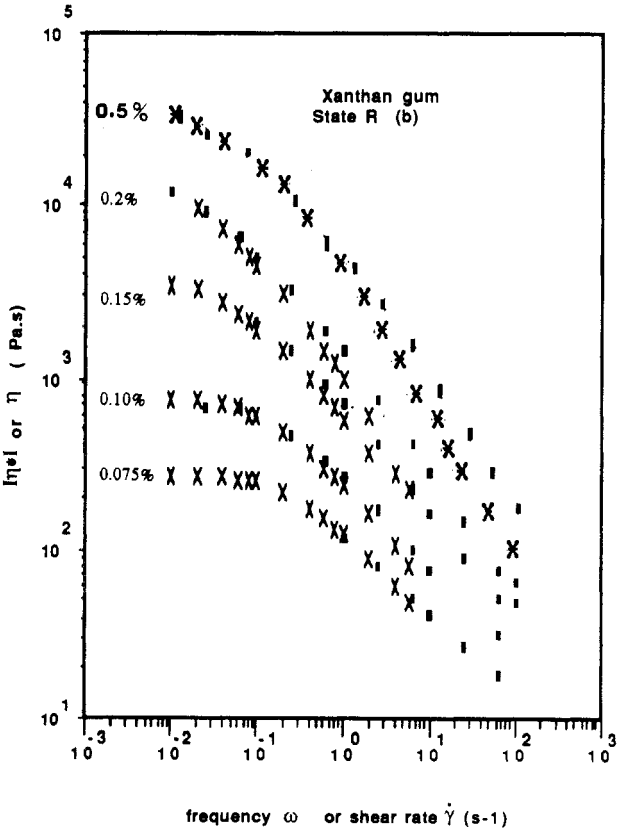

Figure 1. Steady shear viscosity, η (×), and modulus of the complex viscosity, η^* (■), as a function of γ and ω for (a) the native state conformation (N) and (b) the renatured state (R) (T, 25 °C; solvent, NaCl 0.1 M).

is obtained corresponding to the development:

$$\eta_{sp} = C[\eta] + k'(C[\eta])^2 + ... + B(C[\eta])^n$$

When $C[\eta]$ increases, the transition between dilute and semidilute regimes is characterized by a critical concentration C^*; this transition is well characterized by the departure of the curve from the slope 1 when the η_{sp} values are plotted against $C[\eta] + k'(C[\eta])^2$, characterizing the dilute regime. The values obtained for C^* are given in Table I; they are in the range of $C^*[\eta] \sim 1$ as usually found.[15]

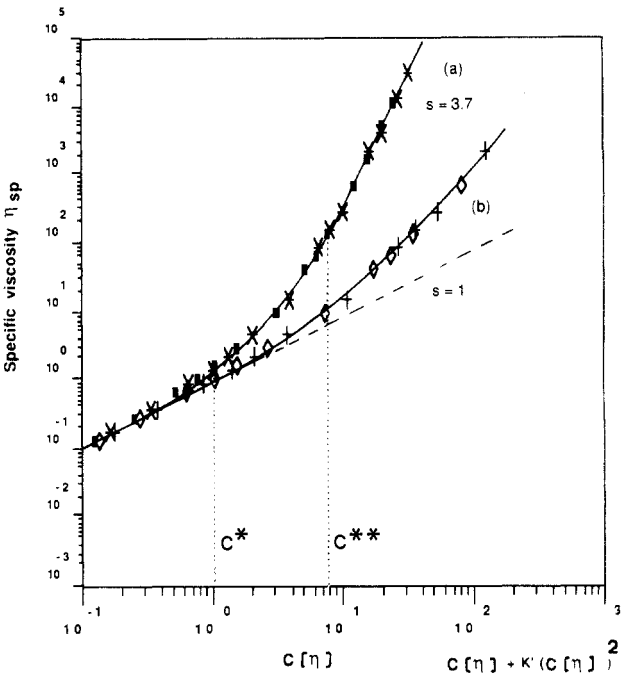

Figure 2. Dependence of the specific viscosity, η_{sp}, as a function of (a) the overlap parameter, $C[\eta]$, and (b) the function $C[\eta] + k'(C[\eta])^2$ for the state N (■ and ◇, respectively) and state R (* and +). The critical concentrations (C^* and C^{**}) and the values of the slopes (s) are indicated. (Same conditions as Figure 1.)

For higher values of $C[\eta]$ (i.e., $C[\eta] > 8$), the dependence of η_{sp} with $C[\eta]$ becomes linear with a slope equal to 3.7 ± 0.3. Consequently, in the higher polymer concentration range, the dependence becomes

$$\eta_{sp} \sim C^{3.7}[\eta]^{3.7} \text{ or } C^{3.7}M^4$$

considering the Mark–Houwink parameter a = 1.1 for xanthan in 0.1 M NaCl.[14] The experimental values obtained for C^{**}, such as $C^{**}[\eta] = 8$, are given in Table I.

These results are in good agreement with works on many synthetic polymers and polysaccharides. The experimental values of the critical concentrations C^* and C^{**} fit quite well with theoretical predictions based on space-filling considerations: $0.7 < C^*[\eta] < 1.5$ and $C^{**}[\eta]_\Theta = 6.14$.[16] The difference between this last value and our result, $C^{**}[\eta] \sim 8$, can be attributed to chain contraction occurring when polymer concentration increases up to the Θ state in the concentrated domain; this effect is not considered in the plot as a function of $C[\eta]$ in which $[\eta]$ is taken as the experimental value for infinite dilution. So, $C[\eta] \sim 8$ characterizes the threshold of the linear dependence of log η_{sp} with log $C[\eta]$ but also the value after which a divergence to the Martin equation[16] $\eta_0 - \eta_s = \eta_s C[\eta] \exp(k''C[\eta])$ is observed. This limit $C[\eta] \sim 8$ introduces a transition from the semidilute regime to a concentrated regime characterized by a uniform segment density in solution[16] where free-draining behavior becomes predominant. In this last domain, the behavior looks like that of a melt. Then, for linear polymers interacting by purely topological entanglements, de Gennes[17,18] has predicted that $\eta \sim M^3C^4$ for polymer solu-

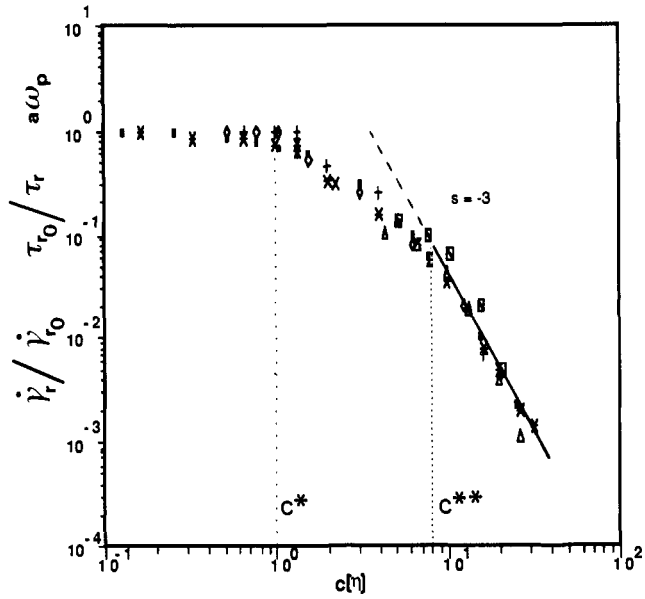

Figure 3. Reduced value of the shear rate corresponding to the transition from Newtonian to pseudoplastic behavior ($\dot{\gamma}_r/\dot{\gamma}_{ro}$) and reduced relaxation time, τ_{ro}/τ_r, estimated in the Rouse model as a function of the overlap parameter for the state N (■ and ◊, respectively) and for the state R (* and +). $a\omega_p$ is also represented for the native state N (⧅) and the renatured state R (△) (a frequency shift factor).

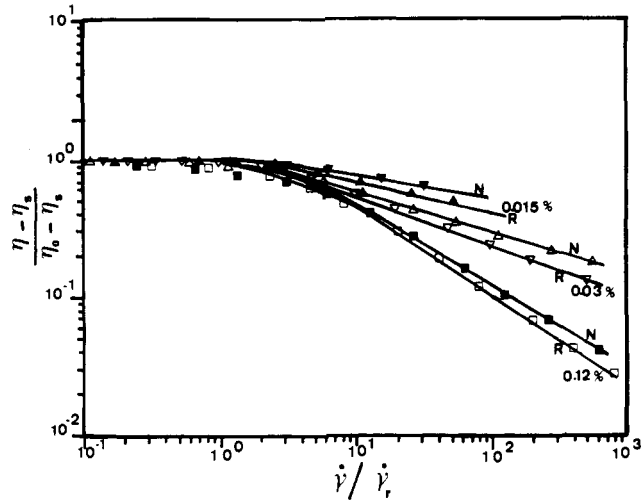

Figure 4. Reduced viscosities as a function of the reduced shear rate for xanthan solutions in the renatured (R) and native (N) conformations at different concentrations.

tion in absence of hydrodynamic interactions and in Θ conditions, which agrees well with that observed experimentally. Previously, $C^{3.3}$ dependence has been reported above $C[\eta] \sim 4$ for random coil polysaccharide solutions.[19] Nevertheless, higher exponents, characteristic of more specific polymer–polymer interactions, have been obtained on xanthan[9] or guar galactomannan.[20] The dependence on M cannot be discussed as we have used only one xanthan molecular weight. Then, our results show that, in the range of concentration investigated here (lower than 2.5 g/L), no specific interactions exist between xanthan chain segments in addition to normal topological entanglements, similar to other polysaccharides[19] but in contrast to previous data published on commercial pasteurized samples of xanthan.[6-10]

2. Flow Curves. (a) Onset of the Shear Rate–Viscosity Dependence. Considering the curves given in Figure 1, it is shown that the onset of non-Newtonian behavior shifts to higher shear rates with decreasing concentration. The transition from Newtonian to viscoelastic behavior is characterized by a critical value of the shear rate, $\dot{\gamma}_r$, usually considered as the longest relaxation time of the Rouse spectrum for the polymeric solution. For low polymer concentrations, a limiting value is reached independent of the concentration ($\dot{\gamma}_{ro}$). The $\dot{\gamma}_{ro}$ value is equal to about 11 ± 2 s^{-1}. Due to imprecision on its determination, it was not possible to find a difference between the two xanthan conformations.

To generalize this behavior, a reduced form was adopted in which $\dot{\gamma}_r/\dot{\gamma}_{ro}$ is plotted as a function of $C[\eta]$ (Figure 3). The departure from one is located at $C^*[\eta] \sim 0.8$ slightly lower than the overlap concentration C^* determined from the Newtonian values in Figure 2.

With the assumption that the shear-rate dependence of viscosity is caused by a progressive decrease in the steady-state entanglement density, a relaxation time, τ_{ro}, can be defined as[12,16]

$$\tau_{ro} = 6\eta_s[\eta]M/\pi^2RT$$

where R is the gas constant, T the absolute temperature, M the molecular weight, and η_s the solvent viscosity and $6/\pi^2$ is derived from the Rouse model of polymer dynamics. For finite concentrations $[\eta]$ is replaced by $(\eta_o - \eta_s)/\eta_s C$ and thus

$$\tau_r = 6(\eta_o - \eta_s)M/\pi^2CRT$$

with η_o the viscosity of the solution in the Newtonian regime.

The ratio of the calculated values τ_{ro}/τ_r is reported in Figure 3 as a function of $C[\eta]$; it is in good agreement with the experimental $\dot{\gamma}_r/\dot{\gamma}_{ro}$ ratio, indicating that the entanglement concept alone can explain the change of the onset of viscoelastic behavior with polymer concentration. One consequence of the agreement between τ_{ro}/τ_r and $\dot{\gamma}_r/\dot{\gamma}_{ro}$ is the possible reduction of the shear rate $\dot{\gamma}$ either by $\dot{\gamma}_r$ (i.e., $\dot{\gamma}/\dot{\gamma}_r$) or by use of the generalized reduced shear rate β ($\beta = \tau_r\dot{\gamma}\pi^2/6$).[16] This generalized reduced shear rate has been already used with success to reduce viscosity data on guar galactomannan[20] or polystyrene.[16] Reduced curves $(\eta - \eta_s)/(\eta_o - \eta_s) = f(\dot{\gamma}/\dot{\gamma}_r$ or $\beta)$ have been obtained in both cases. An example is given in Figure 4. When $C[\eta]$ increases, the slope of the curve log $\dot{\gamma}_r/\dot{\gamma}_{ro}$ or log $\tau_{ro}/\tau_r = f(\log C[\eta])$ (Figure 3) reaches a limiting value equal to −3 ± 0.3. The expected value for τ_{ro}/τ_r is −2.7 from the dependence of $\eta_{sp} = f(C[\eta])$, and if we equilibrate $1/\dot{\gamma}_r$ to a longest relaxation time using the reptation concept,[18,21,22] the exponent should be contained between −1.75 (good solvent) and −3 (Θ solvent). The experimental value is compatible with the latter value. As recalled previously, when the polymer concentration increases, Θ conditions are approached. This is perhaps at the origin of the agreement found here. Finally, it is worth noticing that the differences between the native and renatured xanthan are contained in the parameter $C[\eta]$.

(b) Dependence of the Non-Newtonian Shear Viscosity on Shear Rate. For $\dot{\gamma} > \dot{\gamma}_r$, the viscosity data take a power law dependence with $\eta \sim [\dot{\gamma}]^{-n}$, with the slope n a function of polymer concentration (see Figure 1). The values of n are given in Figure 5; the values obtained for xanthan are compared with that of polystyrene[16] as a function of $C[\eta]$. At high concentrations, n approaches −0.8, as observed with several polymers in the melt or in concentrated solutions. For example, a limiting n value equal to −0.79 has been reported for guar galactomannan.[20] These values compare quite well with the value −0.818 predicted from the theory of Graessley

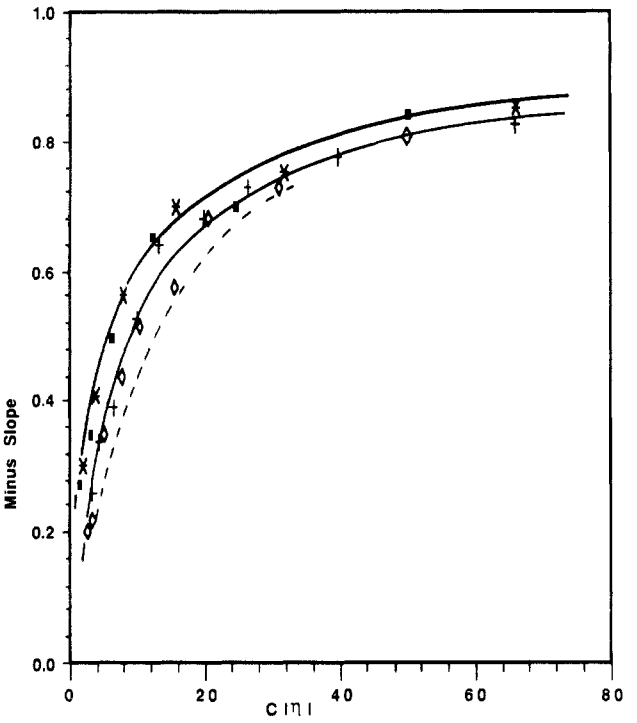

Figure 5. Slopes n in the pseudoplastic domain of $\eta(\dot{\gamma})$ determined on flow curves for states N (■) and R (*). They are compared with the values obtained in dynamic experiments (◊ and +, respectively). See Figure 1; results for polystyrene (- - -).[16]

for monodisperse polymers, knowing that polydispersity of chain length reduces the absolute value of n.[16]

In the range of low $C[\eta]$, the absolute value of n is higher for the stiffer xanthan than for flexible polystyrene. This difference can be attributed to lower hydrodynamic interactions due to the stiffness of the xanthan chain. The behavior of native and renatured xanthans is similar when n is plotted against $C[\eta]$.

3. Dynamic Measurements. Native and renatured ordered conformations were tested in the linear region between 0.166 and 5 g/L. Due to the sensitivity of the rheometer, no measurement was possible in the dilute regime. From these dynamic measurements (i.e., dynamic storage modulus, $G'(\omega)$, and loss modulus, $G''(\omega)$, determinations), the complex dynamic viscosity is given by

$$[\eta^*] = [(G'^2 + G''^2)^{1/2}]/\omega$$

which, using the Cox–Merz rule, can be compared with the steady shear viscosity, $\eta(\dot{\gamma})$, when plotted against radial frequency and shear rate, respectively (Figure 1). At low γ and ω, when the Newtonian plateau is approached, the curves are superposed; then, in the linear viscoelastic domain, the slopes of $[\eta^*(\omega)]$ become slightly lower than that of $\eta(\dot{\gamma})$. This behavior seems original compared with the behavior of flexible polymers for which usually $[\eta^*](\omega) > \eta(\dot{\gamma})$. The values of slopes are compared in Figure 5; no difference is observed between the two structures of xanthan.

The dynamic storage modulus ($G'(\omega)$) and the loss modulus ($G''(\omega)$) versus ω have the general behavior shown in Figure 6; for the renatured conformation $G'(\omega)$ and $G''(\omega)$ cross at a given frequency ω_p, which decreases with increasing polymer concentration, at least above C^*. The change of ω_p (plotted in the reduced form $a\omega_p$) versus the overlap parameter $C[\eta]$ is reported in Figure 3. "a" is an arbitrary shift factor of frequency, to superpose $\omega_p = f(C[\eta])$ curve on the other curves. ω_p appears to follow the same behavior with $C[\eta]$ as $\dot{\gamma}_r$ up to $C[\eta]$ values equal to 30. For higher values of $C[\eta]$, ω_p is shifted toward

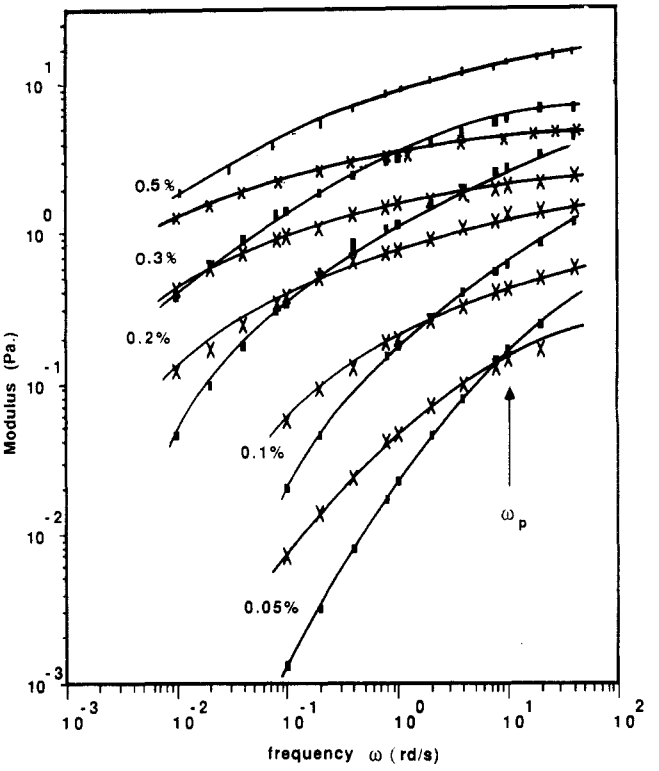

Figure 6. $G'(\omega)$ (■) and $G''(\omega)$ (×) modulus as a function of the frequency, ω, for different polymer concentrations on the renatured state of xanthan.

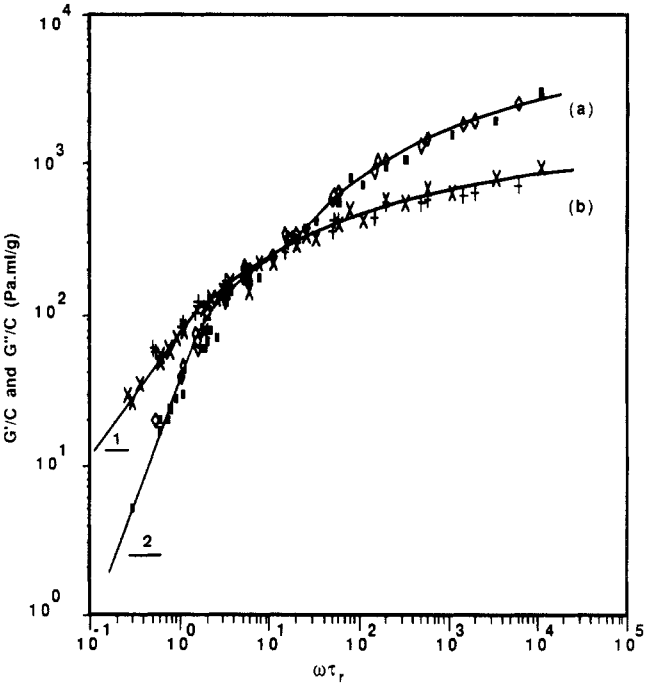

Figure 7. Reduced G' (a) and G'' (b) moduli as a function of the generalized frequency $\omega\tau_r$ on the native state (■ and ×, respectively) and on the renatured state (◊ and +). Xanthan concentrations are from 0.16 to 3 g/L.

lower frequencies and, as for the Newtonian plateau in steady shear experiments, ω_p is no more reached with the equipment used ($\omega_p < 5 \times 10^{-3}$ rad/s). At xanthan concentration lower than C^{**} the ω_p values are too imprecise to confirm the independence of these values as found by Cuvelier and Launay[9] in this range of concentration. However, from the results given in Figures 3 and 7 (where $\omega_p\tau_r$ is found independent of the concentration), it seems that $a\omega_p$ follows the same trend that $\dot{\gamma}_r/\dot{\gamma}_{ro}$ or τ_{ro}/τ_r do;

then, in this case the independence of ω_p with $C[\eta]$ would be only expected in the dilute regime ($C < C^*$). The disagreement with Cuvelier and Launay results[9] is perhaps another consequence of the absence of gellike structure at these concentrations.

The reduced values G'/C and $(G'' - \omega\eta_s)/C$ for C contained between 0.2 and 3 g/L are plotted in Figure 7 as a function of the generalized frequency, $\omega\tau_r$. Similar results are obtained using $\dot{\gamma}_r^{-1}$ instead of τ_r as $\dot{\gamma}_r^{-1} \sim \tau_r$.

All the points are on two generalized curves irrespective of the conformation. So the same shift factor (τ_r or $\dot{\gamma}_r^{-1}$) is applied with success to reduce the shear rate and the frequency. It was not possible to take the G' and G'' reduced values extrapolated to infinite dilution due to the lack of sensitivity of the viscometer. In the range of lower $\omega\tau_r$ values, corresponding also to the lower polymer concentration range, the limit behavior of reduced G'/C and $(G'' - \omega\eta_s)/C$ goes to the slope values 2 and 1, respectively, in agreement with theories;[12] this range corresponds to the Newtonian plateau.

The general aspect of the two curves and the presence of a crossover point above which G'/C becomes higher than G''/C are very similar to the behavior observed in concentrated entangled solutions of polystyrene.[12] Above the crossover frequency, the slopes of both curves decrease without any relation to existing theories. This region, characterized by entanglement coupling is extremely sensitive to chain rigidity and molecular weight distribution; then, the deviation from theoretical previsions given for monodisperse flexible polymers is quite natural. For xanthan concentration higher than 3 g/L, Newtonian plateau, as well as the critical frequency, ω_p, is no more reached, so, it was not possible in these cases to reduce the frequencies and to plot the corresponding curves in Figure 7.

So, Figure 7, obtained on xanthan gum, for polymer concentration up to 3 g/L is characteristic of a polymeric solution with no intermolecular interactions and confirms that the gellike structure of xanthan solutions as described by Ross-Murphy et al.,[7,8] and Cuvelier and Launay,[9] and Rocheford and Middleman[10] is not observed in our solutions, at least for concentrations lower than or equal to 3 g/L ($C[\eta] < 40$).

Conclusion

In this paper, the rheological behavior of an unpasteurized xanthan in the native and renatured conformation is investigated. From flow curves $\eta(\dot{\gamma})$ Newtonian behavior is attained and allows determination of intrinsic and specific viscosities in a large range of $C[\eta]$ values ($C[\eta] < 30$). A generalized curve (Figure 2) is obtained from which two critical polymer concentrations, C^* and C^{**}, are determined. The overlap concentration, C^*, in the order of $[\eta]^{-1}$ limits the dilute regime. The semidilute regime is limited by $C^{**} \sim 8[\eta]^{-1}$, corresponding to the transition to a concentrated domain in which a uniform distribution of segments is suggested. In the concentrated domain, η_{sp} varies following $(C[\eta])^{3.7}$, looking like the behavior of a polymeric melt. This variation agrees quite well with the theoretical prediction for a free-draining solution in Θ conditions. The transition from the Newtonian to the non-Newtonian regime is characterized by a relaxation time, $\dot{\gamma}_r^{-1}$; the dependence of $\dot{\gamma}_r^{-1}$ compared with the calculated values in the Rouse model τ_r is given in terms of $C[\eta]$. In the concentrated domain a general behavior is obtained, whatever conformation is considered, going to a $(C[\eta])^{-3}$ variation following the predicted dependence of chains in Θ state. The results fit with both reptation and Rouse models. The variation of the exponent n of the power law $\eta \sim \dot{\gamma}^{-n}$ is also discussed; the absolute value of n is higher than the value obtained usually for flexible polymers in the intermediate range of $C[\eta]$ but goes to about the same limit around 0.8. From dynamic measurements, it is demonstrated that for low frequency $\eta(\dot{\gamma}) = [\eta^*](\omega)$ as usually assumed following the Cox–Merz rule; for the large values of $\dot{\gamma}$, this relation is no more valid and we obtained $\eta^*(\omega) > \eta(\dot{\gamma})$. The moduli $G'(\omega)$ and $G''(\omega)$ are also considered; the crossover ω_p is found to vary in the same way as $\dot{\gamma}_r$ with $C[\eta]$. Two generalized curves are given for the reduced moduli as a function of the parameter $\omega\tau_r$.

So, both flow and dynamic experimental results are in good agreement to analyze the behavior of the xanthan solution in a large range of polymer concentration (0.2–5 g/L). The structure of the solution at least for xanthan concentrations up to 3 g/L can be described by a classical polymer entanglement mechanism with no predominant hydrodynamic interactions at higher concentrations in contrast with the previous data of the literature. This difference may be due to the nature of the xanthan sample used here whose behavior is known to be different from the heated commercial samples usually studied.

References and Notes

(1) Muller, G.; Lecourtier, J. *Carbohydr. Polym.* **1988**, *9*, 213.
(2) Callet, F.; Milas, M.; Rinaudo, M. *Int. J. Biol Macromol.* **1987**, *9*, 291.
(3) Milas, M.; Rinaudo, M. *Carbohydr. Res.* **1986**, *158*, 191.
(4) Tinland, B.; Rinaudo, M. *Macromolecules* **1989**, *22*, 1863.
(5) Sato, T.; Norisuye, T.; Fujita, H. *Macromolecules* **1984**, *17*, 2696.
(6) Thurston, G. B.; Pope, G. A. *J. Non-Newtonian Fluid Mech.* **1981**, *9*, 69.
(7) Ross-Murphy, S. B.; Morris, V. J.; Morris, E. R. *Faraday Symp. Chem. Soc.* **1983**, *18*, 115.
(8) Richardson, R. K.; Ross-Murphy, S. B. *Int. J. Biol. Macromol.* **1987**, *9*, 257.
(9) Cuvelier, G.; Launay, B. *Carbohydr. Polym.* **1986**, *6*, 321.
(10) Rochefort, W. E.; Middleman, S. *J. Rheol.* **1987**, *31* (4), 337.
(11) Tam, K. C.; Tiu, C. *J. Rheol.* **1989**, *33* (2), 227.
(12) Ferry, J. D. *Viscoelastic Properties of Polymers*, 3rd ed.; Wiley: New York, 1980.
(13) Callet, F.; Milas, M.; Rinaudo, M. *Carbohydr. Polym.* **1989**, *11*, 127.
(14) Milas, M.; Rinaudo, M.; Tinland, B. *Polym. Bull.* **1985**, *14*, 157.
(15) Castelain, C.; Doublier, J. L.; Lefebvre, J. *Carbohydr. Polym.* **1987**, *7*, 1.
(16) Graessley, W. W. *Adv. Polym. Sci.* **1974**, *16*, 1.
(17) de Gennes, P.-G. *Nature* **1979**, *282*, 367.
(18) de Gennes, P.-G. *Macromolecules* **1976**, *9*, 587 and 594.
(19) Morris, E. R.; Culter, A. N.; Ross-Murphy, S. B.; Rees, D. A. *Carbohydr. Polym.* **1981**, *1*, 5.
(20) Robinson, G.; Ross-Murphy, S. B.; Morris, E. R. *Carbohydr. Res.* **1982**, *107*, 17.
(21) de Gennes, P.-G. *J. Chem. Phys.* **1971**, *55*, 572.
(22) Doi, M.; Edwards, S. F. *J. Chem. Soc., Faraday Trans. 2* **1978**, *74*, 1789, 1802, and 1818; **1979**, *75*, 38.